Modeling, Simulation and Control of Matrix Converter for Variable Speed Wind Turbine System

M. Alizadeh Moghadam*, R. Noroozian*(C.A.) and S. Jalilzadeh*

Abstract: This paper presents modeling, simulation and control of Matrix Converter (MC) for Variable Speed Wind Turbine (VSWT) system including Permanent Magnet Synchronous Generator (PMSG). For a given wind speed, the power available from a wind turbine is a function of its shaft speed. To obtain the maximum available power from the wind at different wind speeds, the MC adjusts the PMSG shaft speed. The proposed control system allowing independent control Maximum Power Point Tracking (MPPT) of generator side and regulate reactive power of grid side for the operation of the VSWT system. The MPPT is implemented by a new control system. This control system is based on control of Zero D-axis Current (ZDC). The ZDC control can be realized by transfer the three-phase stator current in the stationary reference frame into d-and q-axis components in the synchronous reference frame. Also, this paper is presented, a novel control strategy to regulate the reactive power supplied by a variable speed wind energy conversion system. This control strategy is based on Voltage Oriented Control (VOC). The simulation results based on Simulink/Matlab software show that the controllers can extract maximum power and regulate reactive power under varying wind velocities.

Keywords: Matrix Converter (MC), Maximum Power Point Tracking (MPPT), Permanent Magnet Synchronous Generator (PMSG), Space Vector Modulation (SVM), Variable Speed Wind Turbine (VSWT).

1 Introduction

Over the last twenty years, renewable energy sources have been attracting great attention due to the cost increase, limited reserves and adverse environmental impact of fossil fuels. In the meantime, technological advancements, cost reduction, and governmental incentives have made some renewable energy sources more competitive in the market. Among them, wind energy is one of the fastest growing renewable energy sources [1]. The energy from the wind turbine system can be connected to a load or to the grid through power electronic converters. The power electronic converters can be used as a DC link converter or matrix converter [2]. MC is a direct frequency converter, which does not require any element of energy storage. When compared with a conventional two-stage ac/dc/ac converter, the MC has some important advantages. For instance, MC is highly controllable and robust due to absence of components such as electrolytic capacitors [3].

Various types of generators can be used for wind turbines. The generators include the Squirrel Cage Induction Generator (SCIG), the Doubly Fed Induction Generator (DFIG), the Wound Rotor Synchronous Generator (WRSG) and the Permanent-Magnet Synchronous Generator (PMSG) [4].

A VSWT system with a DFIG, using an MC in the rotor circuit has been presented in [5]. In this system, the MC is used to control the DFIG based on a sliding mode control technique to extract the maximum energy from the wind. A field oriented vector control method is used in [6] to control a Brushless Doubly-Fed Machine (BDFM) in order to capture maximum wind energy and improve the generated electric power quality. A VSWT system with SCIG and MC is used to control the MPPT in [7, 8]. PMSG has received much attention in wind energy conversion because of the absence of the rotor windings, a high power density can be achieved, reducing the size and weight of the generator. In addition, there are no rotor winding losses, reducing the thermal stress on the rotor [9]. Using matrix converter with PMSG due to lower volume and more flexible structure, with minimal maintenance costs to other structures, it is the best option for micro grid and local applications [4, 10].

Iranian Journal of Electrical & Electronic Engineering, 2015.
Paper first received 01 Sep. 2014 and in revised form 21 Apr. 2015.
* The Authors are with the Department of Electrical Engineering, University of Zanjan, Zanjan, Iran.
E-mails: m.alizadehmoghadam@yahoo.com, noroozian@znu.ac.ir and jalilzadeh@znu.ac.ir.

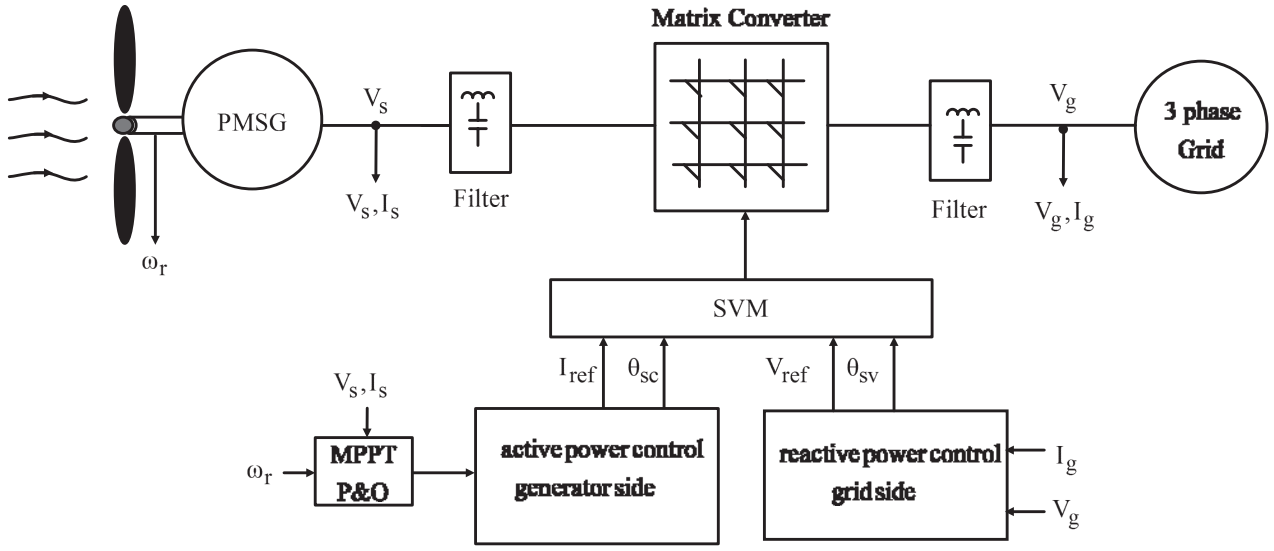

Fig. 1 Wind Energy Conversion System with Matrix Converter

In order to control the MPPT wind turbine system, various algorithms have been proposed in [11-13]. Within different algorithms for MPPT, three famous methods are: Wind Speed Measurement (WSM) [14], Perturbation and Observation (P&O) [15] and Power Signal Feedback (PSF) [16]. The P&O method is proper for wind turbines with small inertia, but not for medium and large inertia wind turbine systems. In the P&O method, the wind turbine speed is varied in small steps and the corresponding change in power is observed [15].

In this paper, the modeling and control of MC for VSWT system has been presented. The aim of this paper is control the MPPT of VSWT system and regulate reactive power delivery to grid. The proposed control system is implemented by space vector modulation technique for switching MC. The results of the digital simulation show that the proposed system can extract maximum power and also regulate reactive power under varying wind velocities.

In the next section, the wind turbine system components are introduced. In section 3 structure of three-phase to three-phase MC is presented. Control system for implementation MPPT and regulate reactive power are presented in Section 4. Finally, simulation and conclusions are presented in Sections 5 and 6, respectively.

2 Model of System Components

Fig. 1 shows the block diagram of VSWT system including wind turbine, PMSG, MC, and utility grid. For this topology, the proposed control system allowing independent control MPPT of generator side and regulate reactive power of grid side. In the following the components of model will be described.

2.1 Dynamic Model of Wind Turbine

The energy in the wind with passing through turbine blades convert to mechanical torque. It is transmitted to the generator with the turbine shaft. Power delivered with wind turbine is dependent to wind density, the area is swept with the blades and the cube of the wind speed. The output mechanical power of the wind turbine shaft can be expressed as follows [8]:

$$P_T = 0.5 C_p \rho A V_w^3 \quad (1)$$

where ρ is the air density (in kilograms per cubic meter), C_P is the power coefficient (dimensionless), A (πR_r^2) is the blade swept area of the turbine (in square meters), R_r is the radius of the turbine shaft (in meters), V_W is the wind speed (in meters per second), and P_T is the wind turbine mechanical power (in watts). Also, C_P is a function of λ (tip-speed ratio) and β (pitch angle), and is given by [17].

$$C_P(\lambda,\beta) = 0.73\left[\frac{151}{\lambda_i} - 0.58\beta - 0.002\beta^{2.14} - 13.2\right] e^{-\frac{18.4}{\lambda_i}} \quad (2)$$

where

$$\lambda_i = \left(\frac{1}{\lambda - 0.02\beta} - \frac{0.003}{\beta^3 + 1}\right)^{-1} \quad (3)$$

with

$$\lambda = \frac{\omega_r R}{Vw} \quad (4)$$

in which ω_r is the rotational speed of turbine rotor (in radians per second). The coefficient C_P signifies the part of wind energy, which is converted to mechanical energy by the wind turbine. According to Eq. (1) the amount of power produced by a wind turbine depends

on the turbine speed, turbine parameters and air density. The air density is usually assumed to be constant. Also the turbine parameters are specified by the designer and constants too.

2.2 Dynamic Model of PMSG

In the PMSG, the rotor magnetic flux is generated by permanent magnets, and this generator is brushless. Because of the absence of the rotor windings, a high power density can be achieved, reducing the size and weight of the generator. In addition, there are no rotor winding losses, reducing the thermal stress on the rotor. Dynamic model of PMSG in the synchronous reference frame can be expressed as follow [18].

$$V_{ds} = -R_s i_{ds} - L_d \frac{di_{ds}}{dt} + \omega_r L_q i_{qs} \tag{5}$$

$$V_{qs} = -R_s i_{qs} - L_q \frac{di_{qs}}{dt} - \omega_r L_d i_{ds} + \omega_r \lambda_r \tag{6}$$

where R_s is the stator winding resistance, L_d, L_q are the stator dq-axis self-inductances, ω_r is the rotor speed in the synchronous reference frame, λ_r is the rotor flux-linkage, i_{ds}, i_{qs} and V_{ds}, V_{qs} are the dq-axis stator currents and the dq-axis stator voltages, respectively. The electromagnetic torque produced by the PMSG can be expressed as follow [18]:

$$T_e = (\frac{3}{2})P[\lambda_r i_{qs} - (L_d - L_q) i_{ds} i_{qs}] \tag{7}$$

where P is pairs poles of PMSG.

2.3 Drive Train

In this paper, the VSWT system is represented with the two mass drive train model. The differential equations governing it can be expressed as follows [18]:

$$2H_{tur} \frac{d\omega_{tur}}{dt} = T_{tur} - K_s \theta_s - D_s(\omega_{tur} - \omega_r) \tag{8}$$

$$2H_{gen} \frac{d\omega_r}{dt} = K_s \theta_s - T_{gen} + D_s(\omega_{tur} - \omega_r) \tag{9}$$

$$\frac{d\theta_s}{dt} = \omega_{tur} - \omega_r \tag{10}$$

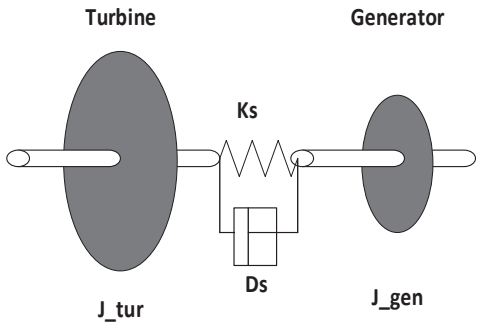

Fig. 2 Two-mass drive train model.

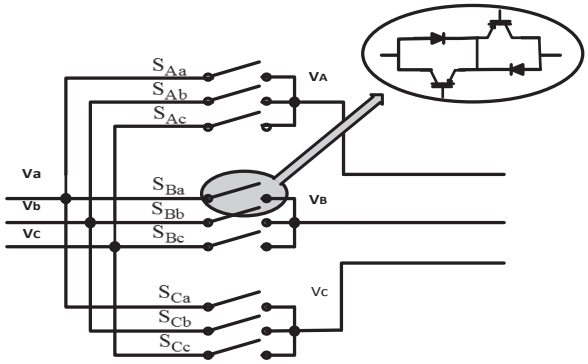

Fig. 3 Matrix converter, three phase to three phase.

where H_{tur} is the inertia constant of the turbine, H_{gen} is the inertia constant of the PMSG, θ_S is the shaft twist angle, ω_{tur} is the angular speed of the wind turbine in p.u., ω_r is the rotor speed of the PMSG in p.u., K_S shaft stiffness and D_S is damping coefficient. Fig. 2 shows the two mass drive train model.

3 Matrix Converter

Matrix Converter was first introduced in the work of Venturini and Alesina in 1980 [19]. The MC provides direct ac/ac conversion, which does not require any energy storage element. Absence of bulky capacitors in the structure of this converter results in reduced size and improved reliability compared to conventional two-stage ac/dc/ac frequency converters [7].

MC is a single stage converter with 18 bidirectional power switches that connects three-phase voltage source to three-phase load [2], [12]. The MC topology is composed of an array of nine bidirectional switches connecting each phase of input to each phase of the output, as shown in Fig. 3. Due to the MC is supplied by the voltage source, the input phases must never be shorted, and due to the inductive nature of load, the output phases must not be left open. If the switching function of a switch, S_{jk} in Fig. 3, is defined as:

$$S_{jk} = \begin{cases} 1, & S_{jk} \text{ closed} \\ 0, & S_{jk} \text{ open} \end{cases} \quad j \in \{A, B, C\},\ k \in \{a, c, d\} \tag{11}$$

The constrains can be expressed as:

$$S_{ja} + S_{jb} + S_{jc} = 1, \qquad j \in \{A, B, C\} \tag{12}$$

The switching combinations according Table 1 can be classified into three groups. The first group of this classification includes six combinations, which each output phase is connected to a different input phase. In second group, there are 3×6=18 combinations with two output phases shorted. The third group includes three combinations with all three output phases shorted.

The switching is based on the Indirect Matrix Converter (IMC). The IMC emulates a Voltage Source Rectifier (VSR) and Voltage Source Inverter (VSI) conversion. The space vector modulation is simultaneously employed in both VSR and VSI parts.

Table 1 MC Switching Combinations

Group	A B C	V_{AB} V_{BC} V_{CA}	i_a i_b i_c	S_{Aa} S_{Ab} S_{Ac}	S_{Ba} S_{Bb} S_{Bc}	S_{Ca} S_{Cb} S_{Cc}
I	a b c	V_{ab} V_{bc} V_{ca}	i_A i_B i_C	1 0 0	0 1 0	0 0 1
	a c b	$-V_{ca}$ $-V_{bc}$ $-V_{ab}$	i_A i_C i_B	1 0 0	0 0 1	0 1 0
	b a c	$-V_{ab}$ $-V_{ca}$ $-V_{bc}$	i_B i_A i_C	0 1 0	1 0 0	0 0 1
	b c a	V_{bc} V_{ca} V_{ab}	i_C i_A i_B	0 1 0	0 0 1	1 0 0
	c a b	V_{ca} V_{ab} V_{bc}	i_B i_C i_A	0 0 1	1 0 0	0 1 0
	c b a	$-V_{bc}$ $-V_{ab}$ $-V_{ca}$	i_C i_B i_A	0 0 1	0 1 0	1 0 0
II-A	a c c	V_{ca} 0 V_{ca}	i_A 0 $-i_A$	1 0 0	0 0 1	0 0 1
	b c c	V_{bc} 0 $-V_{bc}$	0 i_A $-i_A$	0 1 0	0 0 1	0 0 1
	b a a	$-V_{ab}$ 0 V_{bc}	$-i_A$ i_A 0	0 1 0	1 0 0	1 0 0
	c a a	V_{ca} 0 $-V_{ca}$	$-i_A$ 0 i_A	0 0 1	1 0 0	1 0 0
	c b b	$-V_{bc}$ 0 V_{bc}	0 $-i_A$ i_A	0 0 1	0 1 0	0 1 0
	a b b	$-V_{ab}$ 0 V_{ab}	i_A $-i_A$ 0	1 0 0	0 1 0	0 1 0
II-B	c a c	V_{ca} $-V_{ca}$ 0	i_B 0 $-i_B$	0 0 1	1 0 0	0 0 1
	c b c	$-V_{bc}$ V_{bc} 0	0 i_B $-i_B$	0 0 1	0 1 0	0 0 1
	a b a	V_{ab} $-V_{ab}$ 0	$-i_B$ i_B 0	1 0 0	0 1 0	1 0 0
	a c a	$-V_{ca}$ V_{ca} 0	$-i_B$ 0 i_B	1 0 0	0 0 1	1 0 0
	b c b	V_{bc} $-V_{bc}$ 0	0 $-i_B$ i_B	0 1 0	0 0 1	0 1 0
	b a b	$-V_{ab}$ V_{ab} 0	I_B $-i_B$ 0	0 1 0	1 0 0	0 1 0
III-C	c c a	0 V_{ca} $-V_{ca}$	i_C 0 $-i_C$	0 0 1	0 0 1	1 0 0
	c c b	0 $-V_{bc}$ V_{bc}	0 i_C $-i_C$	0 0 1	0 0 1	0 1 0
	a a b	0 V_{ab} $-V_{ab}$	$-i_C$ i_C 0	1 0 0	1 0 0	0 1 0
	a a c	0 $-V_{ca}$ V_{ca}	$-i_C$ 0 i_C	1 0 0	1 0 0	0 0 1
	b b c	0 V_{bc} $-V_{bc}$	0 $-i_C$ i_C	0 1 0	0 1 0	0 0 1
	b b a	0 $-V_{ab}$ V_{ab}	i_C $-i_C$ 0	0 1 0	0 1 0	1 0 0
III	a a a	0 0 0	0 0 0	1 0 0	1 0 0	1 0 0
	b b b	0 0 0	0 0 0	0 1 0	0 1 0	0 1 0
	c c c	0 0 0	0 0 0	0 0 1	0 0 1	0 0 1

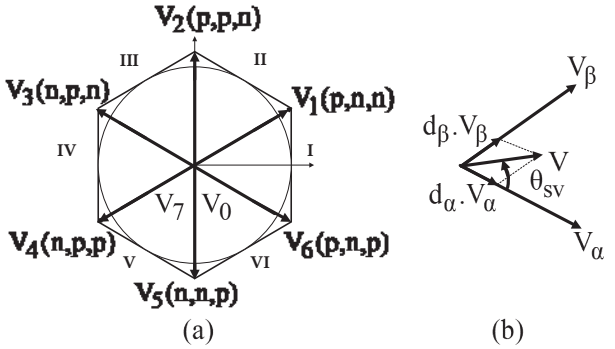

Fig. 4 The space vector modulation of VSI. (a) VSI hexagon, (b) Space vector addition in different sectors.

3.1 VSI Output Voltage SVM

Consider the VSI part of the circuit in Fig. 3 as a standalone VSI, which is supplied by a dc voltage source, $V_{pn} = V_{dc}$. The VSI switches can assume only six allowed combinations which yield nonzero output voltages, and two combinations with zero output voltages. Therefore, the resulting output voltage space vector can be expressed as follows:

$$V = \frac{2}{3}(V_A + V_B\, e^{j120} + V_C\, e^{-j120}) \tag{13}$$

where, can assume only eight discrete value, $V_0 - V_7$ as shown in Fig. 4. The space vector of the desired output voltages can be approximately synthesized by two adjacent switching state vectors, V_α and V_β, and the zero

voltage vector, V_0 or V_7, as shown in Fig. 4. In each sectors the angle between the adjacent switching state vectors is 60°, and the duty cycles of the switching state vectors can be expressed as follow:

$$d_\alpha = T_\alpha / T_s = m_v . \sin(60 - \theta_{sv}) \quad (14)$$

$$d_\beta = T_\beta / T_s = m_v . \sin(\theta_{sv}) \quad (15)$$

$$d_{ov} = T_{ov} / T_s = 1 - d_\alpha - d_\beta \quad (16)$$

where m_v is the VSI modulation index:

$$0 \le m_v = (\sqrt{3}.V_{om}) / V_{dc} \le 1 \quad (17)$$

3.2 VSR Input Current SVM

Consider the VSR part of the circuit in Fig. 3. The VSR input current SVM is completely similar to the VSI output SVM. The VSR hexagon is shown in Fig. 5. The VSR duty cycles are:

$$d_\mu = T_\mu / T_s = m_c . \sin(60 - \theta_{sc}) \quad (18)$$

$$d_v = T_v / T_s = m_c . \sin(\theta_{sc}) \quad (19)$$

$$d_{oc} = T_{oc} / T_s = 1 - d_\mu - d_v \quad (20)$$

where m_c is the VSR modulation index :

$$0 \le m_c = I_{im} / I_{dc} \le 1 \quad (21)$$

3.3 MC Output Voltage and Input Current SVM

To assure proper operation of the converter, the two modulation strategies must now be combined to generate the switching pattern for the entire converter by a product of the corresponding duty cycles.

$$d_{\alpha\mu} = d_\alpha . d_\mu = m . \sin(60 - \theta_{sv}) . \sin(60 - \theta_{sc}) \quad (22)$$

$$d_{\beta\mu} = d_\beta . d_\mu = m . \sin(\theta_{sv}) . \sin(60 - \theta_{sc}) \quad (23)$$

$$d_{\alpha v} = d_\alpha . d_v = m . \sin(60 - \theta_{sv}) . \sin(\theta_{sc}) \quad (24)$$

$$d_{\beta v} = d_\beta . d_v = m . \sin(\theta_{sv}) . \sin(\theta_{sc}) \quad (25)$$

$$d_0 = 1 - d_{\alpha\mu} - d_{\beta\mu} - d_{\alpha v} - d_{\beta v} \quad (26)$$

where $m = m_c . m_v$.

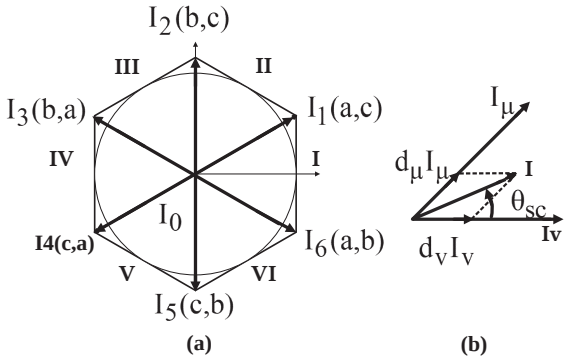

Fig. 5 The space vector modulation of VSR. (a) VSR hexagon, (b) Space vector addition in different sectors.

4 Proposed Control System

The synchronous generator can be controlled by a number of methods to achieve different objectives [5]. In this section introduced Zero D-axis Current (ZDC) control for PMSG and then implemented MPPT algorithm. Also a new control system to regulate the reactive power supplied by a variable speed wind energy conversion system is presented, which is implemented using modulation MC.

4.1 Zero D-axis Current (ZDC) Control

The zero d-axis current control can be realized by resolving the three-phase stator current in the stationary reference frame into dq-axis components in the synchronous reference frame. The d-axis component, i_{ds}, is then controlled to be zero. With the d-axis stator current kept at zero, the stator current is equal to its q-axis component i_{qs} [20].

$$\begin{cases} \vec{i_s} = i_{ds} + j i_{qs} = j i_{qs} \\ i_s = \sqrt{{i_{ds}}^2 + {i_{qs}}^2} = i_{qs} \end{cases} , \quad i_{qs} = 0 \quad (27)$$

where $\vec{i_s}$ is the stator current space vector and is represents its magnitude, which is also the peak value of the three-phase stator current in the stationary reference frame. As a result, the electromagnetic torque of PMSG as follows:

$$Te = \frac{3}{2} P \lambda_r i_{qs} = \frac{3}{2} P \lambda_r i_s \quad (28)$$

where P is the pole pairs and λ_r is the rotor flux linkage produced by permanent magnets in the PMSG. The above equation indicates with i_{ds} = 0, the generator torque is proportional to the stator current i_s With a constant rotor flux linkage λ_r, the torque exhibits a linear relationship with the stator current, which is similar to torque production in a DC machine with a constant field flux, where the electromagnetic torque is proportional to the armature current.

4.2 Maximum Power Point Tracking Algorithm

The wind turbine mechanical output power P_T is affected by the ratio of the turbine shaft speed and the wind velocity. Fig. 6 shows a family of typical P_T versus ω_r curves for different wind velocities for a typical system. As seen in this figure, different power curves have different maximum power, or optimal power $P_{T\text{-}opt}$, which can be calculated as follows:

$$T_{opt} = k\omega^2_{r-opt} \quad (29)$$

$$k = 2.10 \times 10^{-3} \rho R^5_r \quad (30)$$

Optimal operating conditions can be achieved by employing an MPPT method is available in [12]. In this paper, P&O method is used to achieve maximum power of wind turbine. The P&O method is based on perturbing the turbine shaft speed in small steps and observing the resulting changes in turbine mechanical power.

The P&O method can be implemented, by checking the signs of $\Delta\omega_T$ and $\Delta P_T/\Delta\omega_T$. The shaft speed will be either incremented $\Delta\omega_T > 0$ in small steps as long as $\Delta P_T/\Delta\omega_T > 0$, or decremented $\Delta\omega_T < 0$ in small steps as long as $\Delta P_T/\Delta\omega_T < 0$. This is continued until the maximum power point is achieved, i.e., $\Delta P_T/\Delta\omega_T = 0$. On the other hand, if incrementing the shaft speed results in $\Delta P_T/\Delta\omega_T < 0$ or decrementing shaft speed results in $\Delta P_T/\Delta\omega_T > 0$, the direction of shaft speed change must be reversed. The flow chart of the P&O method is shown in Fig. 7. Fig. 8 shows the proposed control system for MPPT of VSWT.

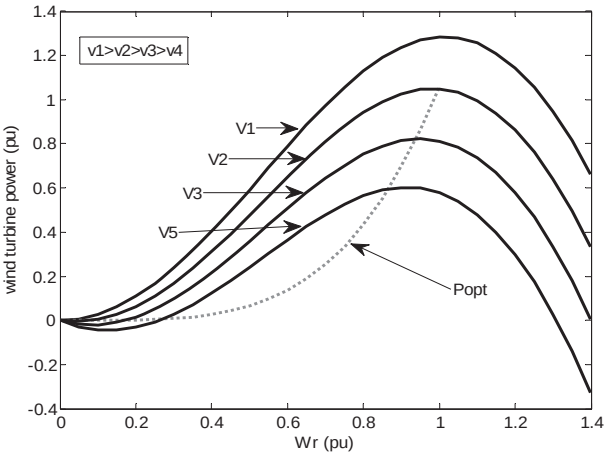

Fig. 6 Wind turbine mechanical output power for wind speed

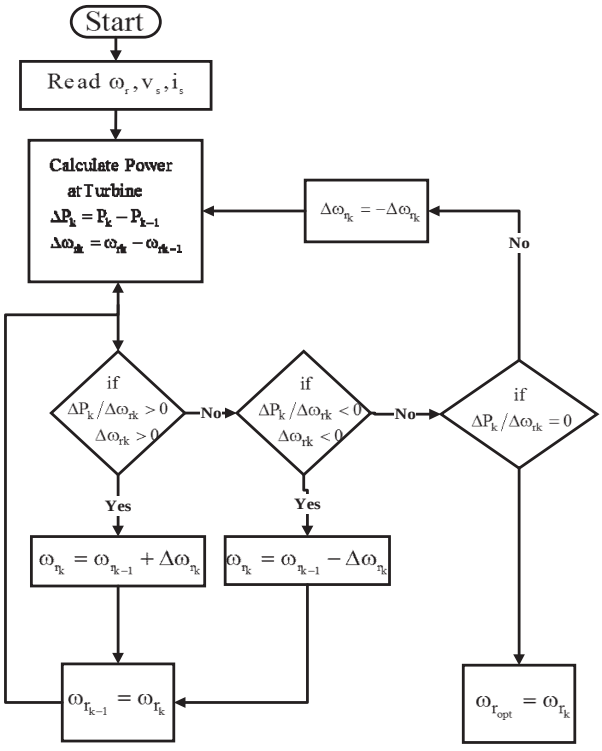

Fig. 7 Flow chart of the P&O method.

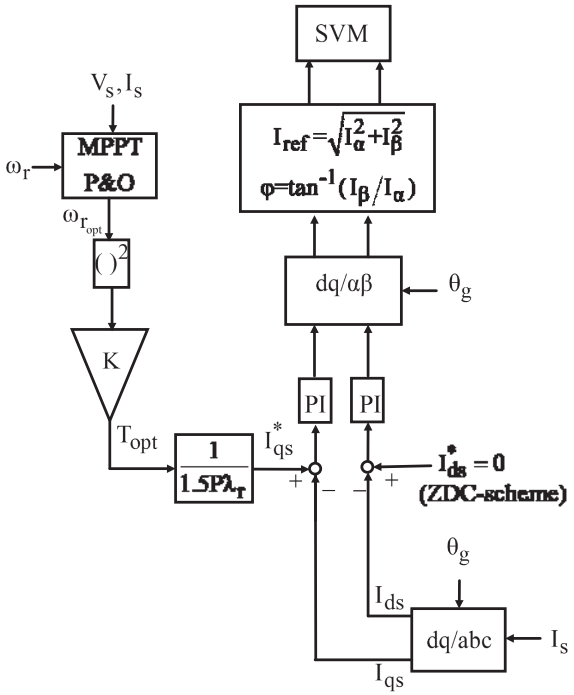

Fig. 8 Proposed control system generator side for MPPT.

4.3 Reactive Power Control System

Most commercial wind turbines deliver the generated power to the electric grid through power converters. The active and reactive power of system delivered to the grid can be calculated by:

$$P_g = 3V_g I_g \cos\varphi \tag{31}$$

$$Q_g = 3V_g I_g \sin\varphi \tag{32}$$

where V_g, I_g and φ, respectively are voltage, current and power factor angle of grid. The grid power factor angle, defined by:

$$\varphi = \angle V_g - \angle I_g \tag{33}$$

The grid power factor can be unity, leading, or lagging. In this section, a new control system to regulate the reactive power supplied by a variable speed wind energy conversion system is presented.

4.3.1 Voltage Oriented Control

The control system is based on Voltage Oriented Control (VOC), which is implemented using modulation MC. To realize the VOC, the grid voltage is measured and its voltage angle is detected for the voltage orientation. This angle is used for the transformation of variables from the abc stationary frame to the dq synchronous frame through the abc/dq transformation or from the synchronous frame back to the stationary frame through the dq/abc transformation. The transformation of the abc variables to the dq frames, referred to as abc/dq transformation, can be expressed in a matrix form:

$$T=\frac{2}{3}\begin{bmatrix} \cos\theta & \cos(\theta-2\pi/3) & \cos(\theta+2\pi/3) \\ -\sin\theta & -\sin(\theta-2\pi/3) & -\sin(\theta+2\pi/3) \end{bmatrix} \quad (34)$$

To achieve the VOC control scheme, the d-axis of the synchronous frame is aligned with the grid voltage vector, therefore the d-axis grid voltage is equal to its magnitude $v_{dg} = v_g$ and the resultant q-axis voltage V_{qg} is then equal to zero ($v_{qg} = \sqrt{v_g{}^2 - v_{dg}{}^2} = 0$), from which the active and reactive powers of the system can be calculated by:

$$P_g = \frac{3}{2} v_{dg} i_{dg} \quad (35)$$

$$Q_g = -\frac{3}{2} v_{dg} i_{qg} \quad (36)$$

The d-axis current and q-axis current references can then be obtained from:

$$i_{dg}^* = \frac{P_g^*}{1.5\ V_{dg}} \quad (37)$$

$$i_{qg}^* = \frac{Q_g^*}{-1.5\ V_{dg}} \quad (38)$$

Fig. 9 shows the proposed control system for regulate reactive power delivery to grid.

5 Simulation Results

To study and analyze the maximum power point tracking and regulate reactive power delivery to grid, the system shown in Fig. 1 has been modeled and simulated by Simulink/Matlab software.

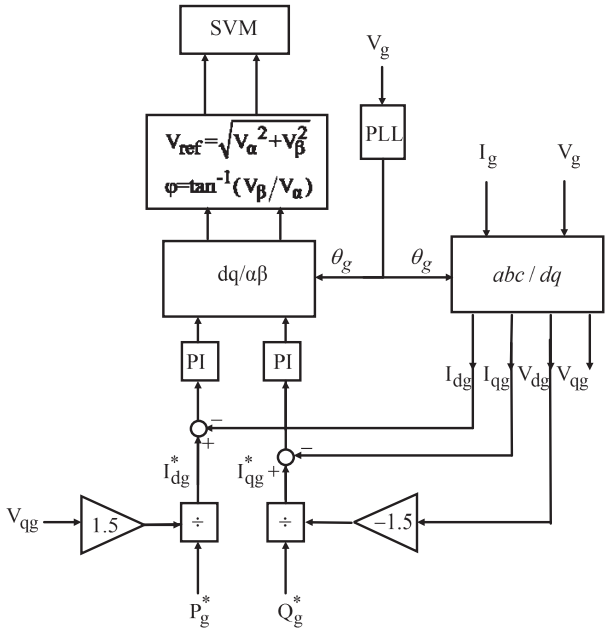

Fig. 9 Proposed control system for regulate reactive power grid side.

The proposed control methods for matrix converter have been modeled using the same software. The simulation results show that the proposed system is able to control MPPT and regulate reactive power for varying wind velocities.

The simulation model of the PMSG based variable speed wind turbine system with three phase to three phase MC (shown in Fig. 1) is modeled by using any arbitrary dq reference frame and data is taken from [14] which are reproduced in Appendix 2. Profile of wind speed step model is shown in Fig. 10. At first, the system is operating at wind speeds 12 m/s. In this wind speed, maximum power is equal 6 kW. In 1 s wind speed of 10 m/s has changed to 12 m/s, also maximum power is equal 4.07 kW. Finally, at 5 second wind speed of 10 m/s has changed to 12 m/s. Again in this wind speed maximum power is equal 6 kW. Accuracy of the MPPT control system to control the active power delivered to the grid is shown in Fig. 11. In each instance, the system follows the wind velocity variations, and the controller leads the system toward the maximum power point based on the mean wind velocity. At the same time the grid reactive power is kept constant by the MC, as shown in Fig. 12.

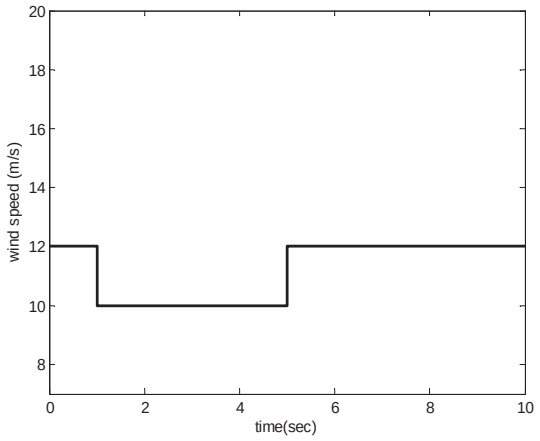

Fig. 10 Wind Speed.

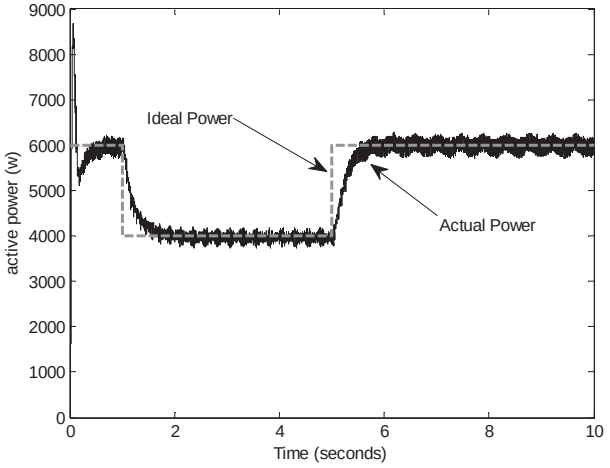

Fig. 11 MPPT control with the P&O method.

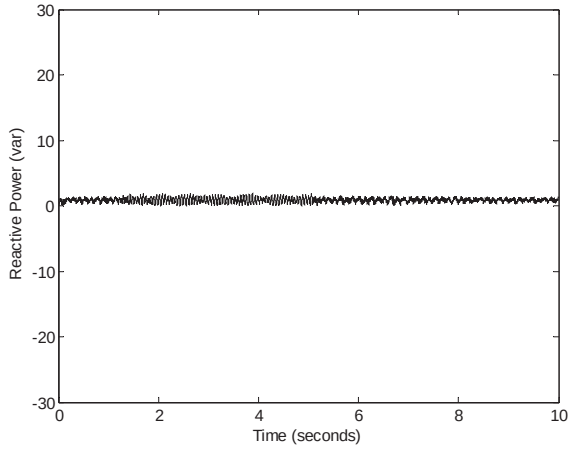

Fig. 12 Grid reactive power during MPPT.

With the implementation of the proposed control circuitry (voltage oriented control) reactive power delivered to the grid is kept at zero. Figs. 13 and 14 shows power coefficient C_P and tip speed ratio λ. It can be found that the λ and C_P are close to the optimal values of 7.05 and 0.44. Fig. 15 shows the variations in the MC input frequency that result in the necessary changes in the PMSG frequency and thus the shaft speed, in attempt to track the maximum power point. Figs. 16 and 17 shows generator torque and turbine torque respectively. Fig. 18 shows the characteristic rotor speed for maximum power point tracking. Fig. 19 shows the characteristic of current phase of the generator for MPPT. The line to line output voltage of the MC including high switching frequency. Due to use the two-order filter has reduced harmonics, as shown in Fig. 20. The simulation results show the capability of structure three-phase to three-phase matrix converter with permanent magnet synchronous generator and proposed control method in tracking the maximum power point and regulate reactive power delivery to grid at varying wind velocities.

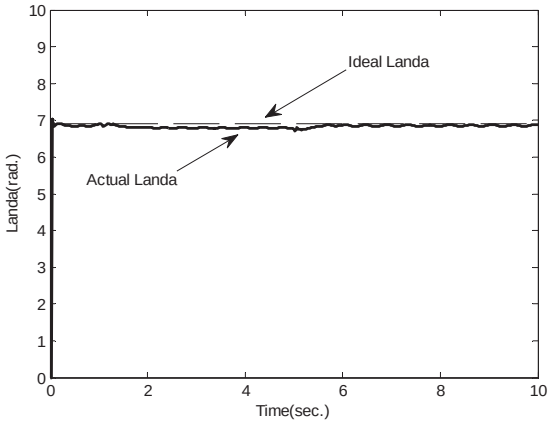

Fig. 13 Tip speed ratio during MPPT.

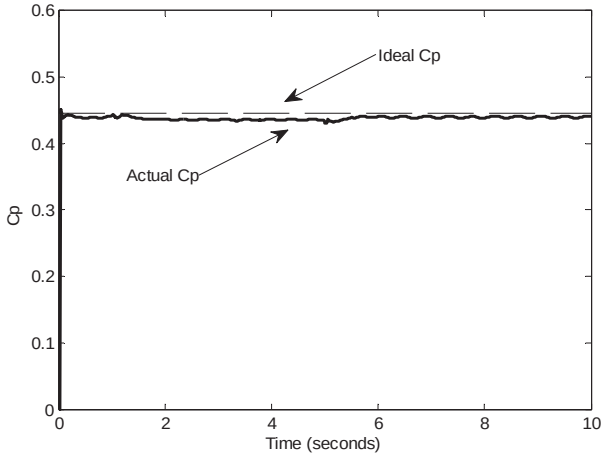

Fig. 14 Power coefficient during MPPT.

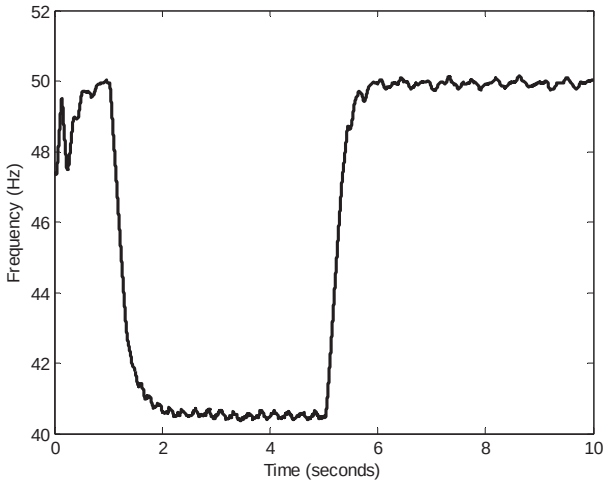

Fig. 15 Frequency variations during MPPT.

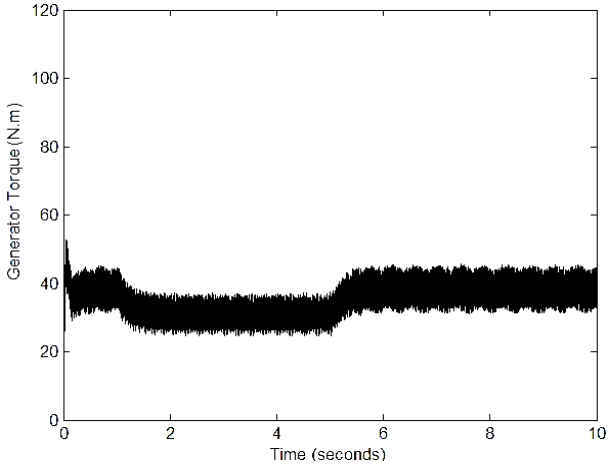

Fig. 16 Generator torque for maximum power point tracking.

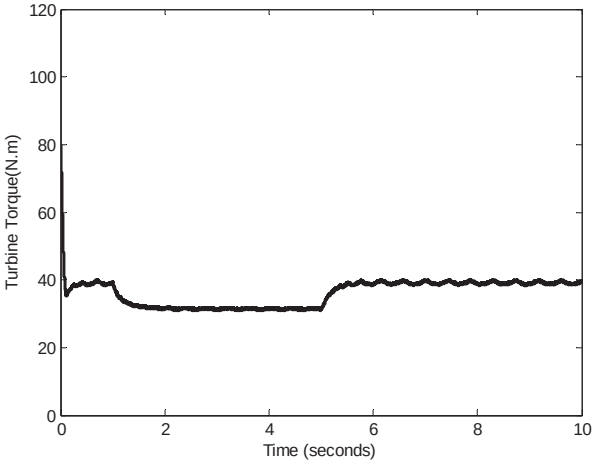

Fig. 17 Turbine torque for maximum power point tracking.

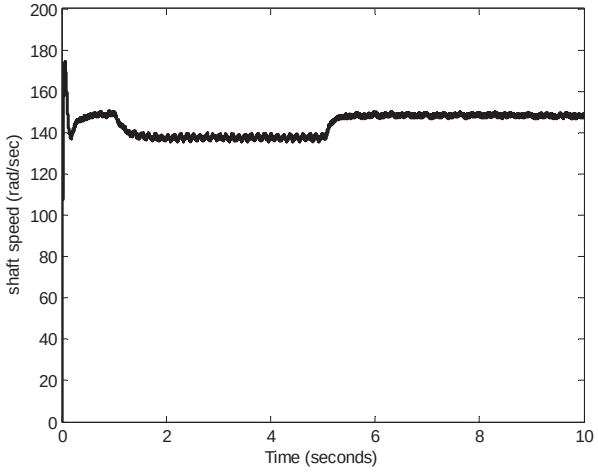

Fig. 18 Generator speed for MPPT.

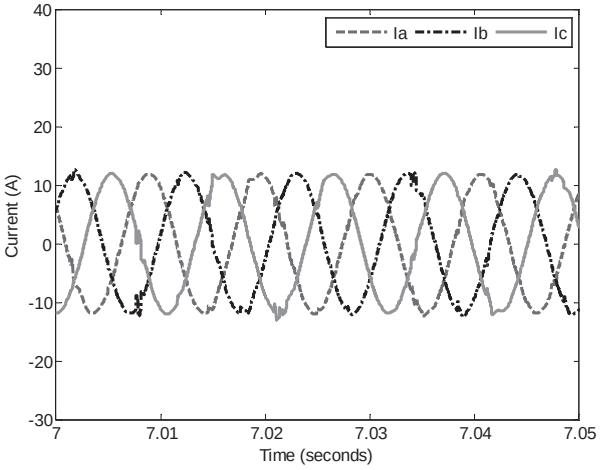

Fig. 19 Current phase generator.

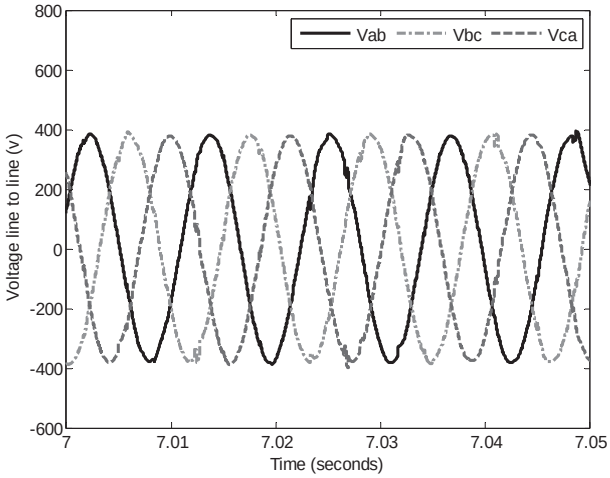

Fig. 20 Instantaneous line voltage.

6 Conclusion

In this paper, three-phase to three-phase matrix converter with permanent magnet synchronous generator was used to connect the variable speed wind turbine to the grid. This paper demonstrates the control MPPT and regulate reactive power are available by controlling the switching of MC. The switching matrix converter was implemented based on space vector modulation. Indirect space vector modulation was used for switching matrix converter. In this paper Simulink/Matlab software has been used for the modeling and the simulation of the system component and proposed control strategies for matrix converter.

Also, the ZDC strategy was implemented with P&O algorithm for MPPT. The VOC is used for control reactive power delivery to grid. The results show that the proposed strategies provide the suitable dynamic behavior for variable speed wind turbine system. Also simulation results show the proposed strategies successful tracking of maximum power and regulate reactive power delivery to grid at varying wind velocities.

Appendix 1

To determine the shaft speed corresponding to MPPT for a particular wind speed, Eq. (1) is differentiated with respect to the shaft speed and equated to zero assuming the turbine radius and air density to be constants. These yields can be expressed as fallow:

$$\frac{dp_T}{d\omega_r}=0.5\rho AV_w^3\frac{dc_p}{d\lambda_i}\frac{d\lambda_i}{d\omega_r} \tag{39}$$

Differentiating Eq. (2) with respect to λ_i, assuming the blade pitch angle β is constant, yields:

$$\frac{dc_p}{d\lambda_i}=\left[\frac{-110.23}{\lambda_i^2}+\frac{2028.23}{\lambda_i^3}-\frac{13.43\psi}{\lambda_i^2}\right]e^{-18.40/\lambda_i} \quad (40)$$

where

$$\psi=0.58+0.002\beta^{2.14}+13.2 \quad (41)$$

Differentiating Eq. (3) with respect to ω_r gives:

$$\frac{d\lambda_i}{d\omega_r}=\frac{V_w R_r[\eta(\beta^3+1)-0.003\sigma]}{(V_w\eta-0.003R\omega_r)} \quad (42)$$

where

$$\sigma=0.02(1+\beta^3)\beta \quad , \quad \eta=1+0.00006\beta+\beta^3 \quad (43)$$

Using Eqs. (33), (34), we have:

$$\frac{dp_T}{d\omega_r}=0.5\rho AV_w^3\left[\frac{-110.23}{\lambda_i^2}+\frac{2028.23}{\lambda_i^3}-\frac{13.43\psi}{\lambda_i^2}\right] .e^{-18.40/\lambda_i}\frac{d\lambda_i}{d\omega_r} \quad (44)$$

At MPPT, $dP_T/d\omega_r=0$. Applying this condition to Eq. (9) provides the value of shaft speed corresponding to the MPP ($\omega_{r\text{-}opt}$), as follows:

$$\omega_{r\text{-}opt}=\frac{V_w}{R_r}\left[\frac{2038.23\eta+\sigma(110.23+13.40\psi)}{(\beta^3+1)(110.23+13.43\psi)+6.08}\right] \quad (45)$$

Putting $\beta=0$, $\psi=13.2$, $\sigma=0$, and $\eta=1$ gives:

$$\omega_{r\text{-}opt}=\frac{V_w}{R_r}6.91 \quad , \quad \lambda_{opt}=6.91 \quad (46)$$

$$C_{P\text{-}opt}=0.44 \quad , \quad \lambda_{i\text{-}opt};7.05 \quad (47)$$

$$T_{opt}=kw^2_{r\text{-}opt} \quad (48)$$

$$k=2.10\times10^{-3}\rho R^5_r \quad (49)$$

Appendix 2

Table A1 Parameter Turbine.

Base wind speed	12 m/s
Blade radius	2.54 m
Air dendity	1.08 kg/m^3
Blade pitch angle	0 degree
H_{tur}	4 s

Table A2 Parameter PMSG

Number of pole	10
Rated speed	153 red/sec
Stator resistance (Rs)	0.425 Ω
Magnetic flux linkage (λ_r)	0.433 Wb
Stator inductance (L_s)	8.4 mH
Rated torque	40 N.m
Rated power	6 kW
H_{gen}	0.4 s
K_s	0.3
D_s	0.7

References

[1] Y. Xia, K. H. Ahmed and B. W. Williams, "Wind turbine power coefficient analysis of a new maximum power point tracking technique", *IEEE Transactions on Industrial Electronics*, Vol. 60, No. 3, pp. 1122-1132, Mar. 2013.

[2] K. Nishida, T. Ahmed and M. Nakaoka, "A cost effective high efficiency power conditioner with simple MPPT control algorithm for wind power grid integration", *IEEE Transactions on Industry Applications*, Vol. 47, No. 2, pp. 893-900, 2011.

[3] M. N. M. E. Haque and K. M. Muttaqi, "A Novel Control Strategy for a Variable Speed Wind Turbine with a PMSG", *IEEE Transactions on Industrial Application*, Vol. 46, No.1, pp. 331-339, Jan. 2009.

[4] S. M. Barakati, M. Kazerani and X. Chen, "A new wind turbine generation system based on matrix converter", in *Power Engineering Society General Meeting*, Vol. 3, pp. 2083-2089, Jun. 2005.

[5] S. F. Pinto, L. Aparicio and P. Esteves, "Direct controlled matrix converters in variable speed wind energy generation systems power engineering", *in Proc. Energy and Electrical Drives*, pp. 654–659, Apr. 2007.

[6] H. Keyuan and H. Yikang, "Investigation of a matrix converter excited brushless doubly fed machine wind-power generation system", *in Proc. Power Electronics and Drive Systems*, Vol. 1, pp. 743-748, Nov. 2003.

[7] S. M. Barakati, M. Kazerani, and J. D. Aplevich, "Maximum power tracking control for a wind turbine system including a matrix converter", *IEEE Trans. Energy Convers.*, Vol. 24, No. 3, pp. 705-713, Sep. 2009.

[8] V. Agarwal, R. K. Aggarwal, P. Patidar and Ch. Patki, "A novel scheme for rapid tracking of maximum power point in wind energy generation systems", *IEEE Trans. Energy Convers.*, Vol. 25, No. 1, pp. 228-236, Mar. 2010.

[9] H. Li, Z. Chen and H. Polinder, "Optimization of multibrid permanent magnet wind generator systems", *IEEE Trans. Energy Convers.*, Vol. 24, No. 1, pp. 82-89, Mar. 2009.

[10] R. Ghazi and A. Khajeh, "GA-Based Optimal LQR Controller to Improve LVRT Capability of DFIG wind turbines", *Iranian Journal of Electrical & Electronic Engineering*, Vol. 9, No. 3, pp. 167-176, 2013.

[11] T. Thiringer and J. Linders, "Control by variable rotor speed of a fixed pitch wind turbine operating in a wide speed range", *IEEE Trans. Energy Convers.*, Vol. 8, No. 3, pp. 520-526, Sep. 1993.

[12] Q. Wang and L. Chang, "An intelligent maximum power extraction algorithm for inverter-based variable speed wind turbine systems", *IEEE*

Trans. Power Electron., Vol. 19, No. 5 pp. 1242-1249, Sep. 2004.
[13] E. Koutroulis and K. Kalaitzakis, "Design of a maximum power tracking system for wind-energy-conversion applications", *IEEE Trans. Industrial Electron.*, Vol. 53, No. 2, pp. 486-494, Apt. 2006.
[14] A. G. Khalil and D. C. Lee, "MPPT control of wind generation systems based on estimated wind speed using SVR", *IEEE Trans. Industrial Electron.*, Vol. 55, No. 3, pp. 1489-1490, Mar. 2008.
[15] R. Chedid, F. Mard and M. Basma, "Intelligent control of a class of wind energy conversion system", *IEEE Trans. Energy Convers.*, Vol. 14, No. 4, pp. 1579-1604, Dec. 1999.
[16] M. Hosseinabadi and H. Rastegar, "DFIG Based wind turbines Behavior Improvement during Wind Variations using Fractional Order Control Systems", *Iranian Journal of Electrical & Electronic Engineering*, Vol. 10, No. 4, pp. 314-32, 2014.
[17] F. Blaabjerg, Z. Chan and S. B. Kjaer, "Power electronics as efficient interface in dispersed power generation systems", *IEEE Trans. Power Electron.*, Vol. 19, No. 5, pp. 1184-1194, Sep. 2004.
[18] C. N. Bhende, S. Mishra and S. G. Malla, "Permanent magnet synchronous generator-based standalone wind energy supply system", *IEEE Trans. Sustainable Ener.*, Vol. 2, No.4, pp. 361-373, Oct. 2011.
[19] A. Alesina and M. Venturini, "Solid-state power conversion: A Fourier analysis approach to generalized transformer synthesis", *IEEE Trans. Circuits Syst.*, Vol. 28, pp. 319-330, Apr. 1981.
[20] J. Dai, D. Xu and B. Wu, "A novel control scheme for current-source converter based PMSG wind energy conversion system", *IEEE Trans. Power Electron.*, Vol. 24, No. 4, pp. 963-973, Apr. 2009.

Majid Alizadeh Moghadam was born in Zanjan, Iran in 1988. He received the B.Sc. degree in electrical engineering from Shahid Babee University, Qazvin, Iran, in 2011, and M.Sc. degree in electrical engineering from Zanjan University, Zanjan, Iran, in 2014. His research interests include renewable energy, distributed generation, power system operation, power electronics, and artificial intelligence.

Reza Noroozian (M'09) was born in Iran. He received the B.Sc. degree in power systems from Tabriz University, Tabriz, Iran, in 2000, and the M.Sc. and Ph.D. degrees in electrical engineering from Amirkabir University of Technology, Tehran, Iran, in 2003 and 2008, respectively. He is an Associate Professor with the Department of Power Engineering, The University of Zanjan, Zanjan, Iran. His areas of interest include power electronics, power systems, power quality, integration and control of renewable generation units, custom power, micro grid operation, distributed-generation modeling, as well as operation and interface control.

Saeed Jalilzadeh was born Iran. He received the B.Sc. and M.Sc. degrees in power systems from Tabriz University, Tabriz, Iran, in 1987 and 1991, respectively, and the Ph.D. degree in electrical engineering Iran University of Science and Technology, Tehran, Iran, in 2005. He is an Associate Professor with the Department of Power Engineering, The University of Zanjan, Zanjan, Iran. His areas of interest include power system operation, power systems, power quality, integration and control of renewable generation units, custom power.